Article

Vapor-Fed Cathode Microbial Electrolysis Cells with Closely Spaced Electrodes Enables Greatly Improved Performance

Ruggero Rossi,* Gahyun Baek, and Bruce E. Logan

Read Online

ACCESS | Metrics & More | Article Recommendations | Supporting Information

ABSTRACT: Hydrogen can be electrochemically produced in microbial electrolysis cells (MECs) by current generated from bacterial anodes with a small added voltage. MECs typically use a liquid catholyte containing a buffer or salts. However, anions in these catholytes result in charge being balanced predominantly by ions other than hydroxide or protons, leading to anode acidification. To enhance only hydroxide ion transport to the anode, we developed a novel vapor-fed MEC configuration lacking a catholyte with closely spaced electrodes and an anion exchange membrane to limit the acidification. This MEC design produced a record-high sustained current density of 43.1 ± 0.6 A/m^2 and a H$_2$ production rate of 72 ± 2 LH$_2$/L-d (cell voltage of 0.79 ± 0.00 V). There was minimal impact on MEC performance of increased acetate concentrations, solution conductivity, or anolyte buffer capacity at applied voltages up to 1.1 V, as shown by a nearly constant internal resistance of only 6.8 ± 0.3 mΩ m^2. At applied external voltages >1.1 V, the buffer capacity impacted performance, with current densities increasing from 28.5 ± 0.6 A/m^2 (20 mM phosphate buffer solution (PBS)) to 51 ± 1 A/m^2 (100 mM PBS). These results show that a vapor-fed MEC can produce higher and more stable performance than liquid-fed cathodes by enhancing transport of hydroxide ions to the anode.

KEYWORDS: *hydrogen generation, microbial electrolysis cell, vapor-fed cathode, anion exchange membrane, pH control*
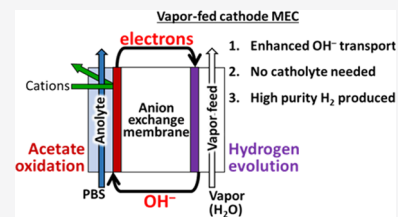
INTRODUCTION

Microbial electrolysis cells (MECs) produce hydrogen gas by coupling a bioanode, generating electrons from the oxidation of organic matter with electrochemical hydrogen evolution at the cathode and an additional power source to provide additional voltage.[1−3] The main advantage of MECs over conventional electrolyzers is the lower energy requirement due to the smaller theoretical voltage input of >0.11 V in MECs compared to >1.2 V for abiotic water electrolysis.[4] In practice, MECs typically operate with an applied voltage ranging from ∼0.6 to 1.2 V, which is still lower than that used for abiotic water electrolysis (∼1.8 V) but larger than the theoretical one. The larger applied potentials are required to overcome overpotentials due to ohmic resistances, sluggish kinetics, and the development of concentration gradients between the electrodes.[5] While the ohmic and kinetic overpotentials can be reduced by diminishing the electrode spacing[6] and improving the activity or the surface area of the catalyst,[7] overpotentials due to concentration gradients require different approaches such as continuous addition of chemicals during operation.[8]

The oxidation of substrate at the anode generates 1 mol of protons per mole of electrons, while an equivalent amount of hydroxide ions are produced at the cathode by the hydrogen evolution reaction (HER) under neutral to alkaline pH conditions.[9] Ideally, if the protons and the hydroxide ions are the only species balancing charge, then the pH neutrality of the solution will be maintained. However, the media typically used in MECs contain ions approximately 10^5 more concentrated than H$^+$/OH$^-$ at pH 7 to maintain a high conductivity of the solution. Thus, ions other than H$^+$/OH$^-$ balance the charge transported between the electrodes, leading to large pH differences between the anode and cathode.[10] If the protons produced at the anode and the hydroxide ions from the cathode are not effectively removed from the electrodes due to preferential transport of other ions, then the anode local pH will decrease and the cathode local pH will increase. These pH changes can occur either in the presence or in the absence (locally) of a membrane separating the electrodes.[5,9,11−13] While the high pH at the cathode is predicted to limit hydrogen production based on thermodynamic potentials for HER using the Nernst equation, in practice, the local cathode pH is a less critical factor than OH$^-$ transport.[5,14,15] Thus, a greater concern than cathode pH is the limited OH$^-$ ion transport to the anode as that will inhibit the activity of the microorganisms responsible for current generation by lowering the anode pH, limiting maximum current densities to only a few A/m^2 or less. Increasing the current density therefore requires operational conditions that

avoid a low anode pH in order to enable industrial production of hydrogen from wastes using MECs.[1,4]

In this study, a novel MEC configuration was developed using a thin anion exchange membrane (AEM) as a solid electrolyte between the electrodes in a membrane electrode assembly (MEA), close-spaced electrodes that avoided gaps between the electrodes and the membrane, and a vapor-fed cathode to avoid ion transport into the cathode that could lead to salt precipitation (Figure 1A,B). Pressing the cathode
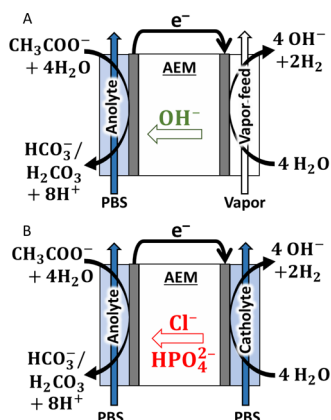

Figure 1. Schematic of the (A) zero-gap MEC configuration with the AEM acting as a solid electrolyte compared to a (B) conventional MEC with a liquid catholyte. Dimensions are not to scale.

against the AEM avoided the need for a catholyte as the ionic conductivity and the water needed for the HER were provided by the close contact with the membrane and a continuous supply of water vapor to the cathode chamber. The small spacing between the electrodes minimized the ohmic resistance by leveraging the high ionic conductivity of the membrane combined with the reduced distance between the electrodes where the H^+/OH^- ions are generated, limiting the transport of ions other than H^+/OH^-. The lack of an aqueous catholyte minimizes salt ion transport into the cathode, which has led to salt precipitation and fouling of previous MECs.[7] This configuration therefore circumvents the development of large concentration gradients that would inhibit anode performance.

◼ MATERIALS AND METHODS

MEC Construction and Operation. The MEC was a double chamber reactor assembled by using two plastic plates with a threaded insert to allow flow into the cell (Figure S1). The anode and cathode chambers were produced by the thickness of the gaskets (3.18 mm), with the chambers separated by an AEM (100 μm, Selemion AMV-N, Asahi), based on a previously described design used for producing electricity in a microbial fuel cell (MFC).[16] The electroactive surface area was 7 cm^2, and the empty MEC volume (anode + cathode chambers) was 4.5 mL, producing a high electrode specific surface area of 157 m^2/m^3. Prior to the MEC assembly, three layers of plastic mesh spacers (S1.5, 30PTFE-625P, Dexmet Corp.) were inserted in the cathode chamber between the cathode and the end plate to maintain a zero-gap spacing between the electrodes, allowing gas to flow past the cathode. Unfortunately, a reference electrode could not be used in this MEC design as insertion of a reference electrode would alter flow paths through the chamber (around the electrode) as well

as impact of continuity of the electric field in the closely spaced electrodes of this MEC.[17−21] Titanium foils (Strem Chemicals Inc.) were used as anode and cathode current collectors. The anode was a 3.18 mm-thick carbon felt (Alfa Aesar) heat-treated at 450 °C for 30 min prior to use.[22] The anode completely occupied the anode chamber, forcing the anolyte to flow through the felt. The impact of the flow rate on the reactor performance has been previously investigated in an MFC using a similar configuration.[23] The cathode catalyst was prepared by spraying a Pt/C ink as previously described.[23] The catalyst ink was sprayed on a bare wet-proofed carbon cloth (Fuel Cell Store), dried overnight under a fume hood at room temperature, and cold (35 °C)-pressed onto the AEM at 4500 psi for 3 min to develop the final MEA.

The anolyte (500 mL) was continuously recirculated at 10 mL/min (theoretical hydraulic retention time, HRT = 14 s). The HRT used for the anode was not substantially different from that previously used in other flow-through MECs,[7,24] and it was kept low to maintain a high substrate concentration for the bioanode.[25] The impact of the HRT on the performance of an MFC with a similar configuration compared with that used here was previously reported to be minor as long as the flow rate was maintained between 2 and 15 mL/min.[23] The anolyte was a 50 mM phosphate buffer solution (PBS, 4.58 g L^{-1} Na_2HPO_4, 2.45 g L^{-1} $NaH_2PO_4 \cdot H_2O$, 0.31 g L^{-1} NH_4Cl, 0.13 g L^{-1} KCl; σ = 7 mS/cm) except as noted. In some experiments, 100 mM PBS (9.15 g L^{-1} Na_2HPO_4, 4.90 g L^{-1} $NaH_2PO_4 \cdot H_2O$, 0.62 g L^{-1} NH_4Cl, 0.26 g L^{-1} KCl; σ = 12 mS/cm) or 20 mM PBS (1.83 g L^{-1} Na_2HPO_4, 0.98 g L^{-1} $NaH_2PO_4 \cdot H_2O$, 0.12 g L^{-1} NH_4Cl, 0.05 g L^{-1} KCl; σ = 4 mS/cm) was used to investigate the impact of the buffer capacity on MEC performance. Sodium acetate was added as the substrate (2 g/L), and the anolyte was amended with trace vitamin and mineral solutions before being fed to the MEC.[26] The anolyte was sparged with N_2 to remove oxygen from the solution for approximately 15 min prior to use. The buffer concentration, substrate type and concentration, and MEC operating conditions were selected based on the most used conditions in the existing MEC literature to allow reproducibility of this study.[27,28] The MECs were operated at 30 °C, and the anolyte was replaced daily except otherwise noted. In one test, the cycle length was increased to 3 days to investigate the stability of the performance and the results of that test are reported in the Supporting Information (Figure S2).

Vapor-Fed MEC. The cathode was fed with vapor from a 15 mL headspace of a sealed glass container filled with deionized water (115 mL). The cathode feed was recirculated at 5 mL/min (HRT = 27 s). The deionized water used to develop a vapor feed at the cathode was never replaced, and it was sparged with N_2 to remove oxygen from the solution for approximately 15 min only prior to startup of the MEC that was started up on day 1.

Liquid-Fed MEC. The liquid catholyte was fed from a 500 mL reservoir. The cathode feed was recirculated at 5 mL/min (HRT = 27 s). In a set of experiments, the cathode was fed with 50 mM phosphate buffer (PB, 4.58 g L^{-1} Na_2HPO_4, 2.45 g L^{-1} $NaH_2PO_4 \cdot H_2O$; σ = 6 mS/cm), 100 mM phosphate buffer (9.16 g L^{-1} Na_2HPO_4, 4.9 g L^{-1} $NaH_2PO_4 \cdot H_2O$; σ = 11 mS/cm), 50 mM KCl (σ = 7 mS/cm), 100 mM KCl (σ = 14 mS/cm), 50 mM KOH (σ = 12 mS/cm; pH = 12.7), or 25 mM HCl (σ = 11 mS/cm; pH = 1.6). The conductivity of the solution used as the catholyte was maintained in a small range between 6 and 12 mS/cm to limit the impact of the solution
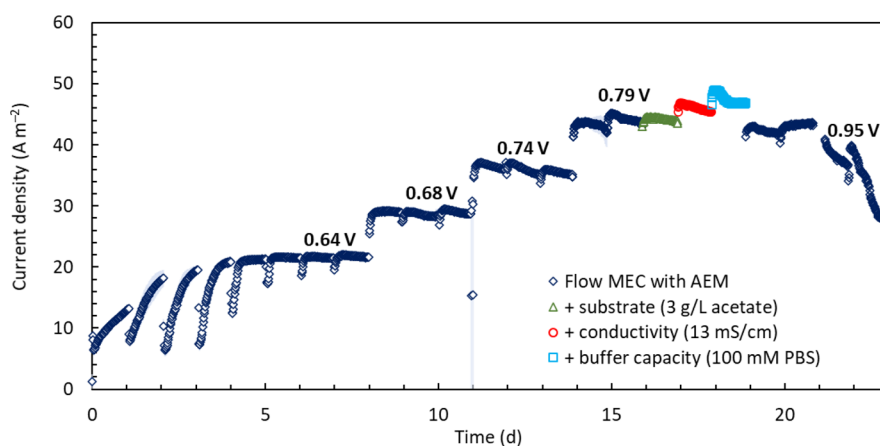
Figure 2. Current density profile over time of the MEC under different cell voltages and operating conditions. Other independent MEC runs are reported in the Supporting Information, showing similar performances at different applied voltages.

conductivity on the performance of the MEC. The initial pH of the PBS and PB solutions was 7.1, while the solutions amended with KCl had a pH of approximately 7.5. The liquid catholytes were replaced daily except otherwise noted and sparged with N_2 to remove oxygen from the solution for approximately 15 min prior to use. The hydrogen accumulated in the gas phase was removed daily with a vacuum pump except as otherwise noted.

Analytical and Electrochemical Measurements. A power supply (3646A, Circuit Specialists) was used to apply a voltage between the anode and cathode. The current was calculated from the voltage drop across a 10 Ω resistor (R_{ext}) connected in series with the MEC. The voltage was measured every 20 min (Keithley 2700) and is reported as the cell voltage (V_{cell}) measured between the anode and cathode and the applied voltage (V_{app}) measured using the monitor output of the power supply. V_{app} includes the R_{ext} used to calculate the current produced by the MEC, while V_{cell} excludes R_{ext}.[29] The current density was normalized by the MEC cross-sectional area (7 cm^2). Variable V_{app} were set during the course of the experiment, ranging from 0.8 to 1.2 V with each voltage applied for at least 24 h. The whole cell performance was analyzed in terms of MEC internal resistance and onset voltage using the electrode potential slope (EPS) method.[29] The solution resistance (R_Ω) was calculated from electrochemical impedance spectroscopy (EIS) by conducting a fast EIS scan at the open circuit voltage (OCV) (from 100 kHz to 500 Hz, 5 mV amplitude, 10 points/decade).[30] EIS was also used to investigate the MEC internal resistance at different cell voltages by applying a sinusoidal voltage perturbation of 5 mV over a frequency range of 1 MHz to 1 mHz at 10 points/decade. The spectra were analyzed with Zfit in the EC-lab software and fitted to an equivalent circuit reported in the Supporting Information. The anode was acclimated in a 28 mL reactor under a potential of 0.0 V vs Ag/AgCl (Basi, Inc.) for at least 2 weeks before being cut to size and installed in the MEC. The electrochemical performance of similar individual anodes and cathodes was previously investigated.[16,23]

The gas produced at the cathode was collected in gas bags (Calibrated Instrument Inc.) installed on the cathode reservoir headspace and analyzed using a gas chromatograph (SRI Instrument) equipped with a molecular sieve column. The gas volume produced was calculated following a previous method[31] and compared with the theoretical H_2 production

rate based on the coulombs produced during each cycle to calculate the cathode faradaic efficiency. The hydrogen production rate was calculated by normalizing the volume of H_2 produced for the overall MEC empty volume of 4.5 mL (anode + cathode chambers). The anode faradaic efficiency was calculated as previously described based on the coulombs produced and the chemical oxygen demand (COD, TNTplus COD reagent; HACH) consumed.[32]

■ RESULTS AND DISCUSSION

Electrochemical Performance at Different Applied Potentials. The vapor-fed cathode MEC produced an average current density over a 24 h cycle of 43.2 ± 1.1 A/m^2 (6.78 A/L) at a V_{cell} of 0.79 ± 0.00 V (V_{app} = 1.1 V) with 2 g/L sodium acetate as a substrate after 15 days of operation (Figure 2). To the best of our knowledge, the current density obtained in this vapor-fed cathode configuration was the highest current (previously 23 A/m^2) at the lowest cell voltage (0.79 vs 1.00 V reported previously) ever reported for an MEC in 50 mM PBS and other media.[5,7,33−35] Three independent runs of a duplicate vapor-fed MECs were tested, all showing similar performances (Supporting Information, Figure S3). A stable current density (± 10%) of 21.7 ± 0.4 A/m^2 over a single cycle (24 h) was generated at a cell voltage of 0.64 ± 0.00 V (V_{app} = 0.8 V). The current density further increased to 29 ± 2 A/m^2 at 0.68 ± 0.02 V (V_{app} = 0.9 V) and to 35.5 ± 0.3 A/m^2 at 0.74 ± 0.00 V (V_{app} = 1.0 V). Increasing V_{app} to 1.2 V decreased the MEC performance, indicating that the maximum current density obtained at V_{app} = 1.1 V was the limiting current density for this configuration and further increasing the applied voltage decreases the MEC performance.[36] It is likely that the limiting current density was due to the development of mass-transfer limitations at the anode, as previously shown in other MEC configurations.[9,12]

The high current density of 43.2 ± 1.1 A/m^2 was enabled by the zero-gap configuration coupled with the AEM and a vapor-fed cathode and not due to the electrode materials (plain carbon felt anode and Pt/C cathode) or anolyte. Higher current densities have been reported for other bioelectrochemical systems only by using dissimilar electrode sizes or anodes operated in three-electrode stirred cells. For example, a peak current density of up to 90 A/m^2 was reported for a single chamber MEC fed with a highly saline electrolyte.[37] However, the current density was calculated by normalization based on

the small cathode area (220 cm^2) compared to the anode (800 cm^2). If the current was normalized by the cathode area, then the maximum current density would have been 25 A/m^2 (40% less than the maximum current density here). A very high current density of 390 A/m^2 was obtained using a three-electrode stirred electrochemical cell designed to minimize mass transfer limitations and improve anodic performance and not to include solution or cathodic energy losses, but it was not tested in an operating bioelectrochemical system that would have had these other internal resistances.[38] The highest current density reported for a flow-through MEC with equally sized electrodes was 22.8 ± 0.1 A/m^2 at a cell voltage of 1.0 V.[7] Even though a lower anolyte buffer capacity was used in that study (10 mM compared to 50 mM here), the solution conductivity was similar to that used here due to a higher salt content (6 mS/cm[34] compared to 7 mS/cm here). The maximum current density was half of that produced here using the vapor-fed cathode MEC and a 27% higher cell voltage. Reducing the MEC voltage enables higher reactor efficiency and reduces the energy input required to produce H$_2$. In other studies from the same group, a maximum current density of 10.2 A/m^2 was reported using 50 mM PBS.[34,35]

Electrochemical Performance at the Use of Different Solution Conditions. The performance of the vapor-fed cathode MEC was further investigated in terms of current density by amending the anolyte with additional substrates, salts (KCl) to increase the conductivity, or 100 mM PBS to increase the buffer capacity (Figure 2 and Figure S5). Increasing the sodium acetate concentration from 2 to 3 g/L did not change the performance of the MEC, producing an average current density of 44.3 ± 0.5 A/m^2 (2 g/L) over a day before amendment compared to 44.2 ± 0.3 A/m^2 after (3 g/L). The impact of using an anolyte amended with KCl to double the anolyte conductivity to 14 mS/cm was larger than that with additional substrates. With additional KCl, the average current density increased by 4% to 46.1 ± 0.5 A/m^2. Using a higher buffer capacity anolyte (100 mM PBS) further increased the average current density by an additional 3% to 47.5 ± 0.8 A/m^2. The improvement in the MEC performance due to additional conductivity and buffer capacity was in line with results previously reported in the literature; however, the increase in performance here was modest compared to that in the literature.[9,12,13,35] Overall, amending the anolyte with additional KCl or PBS increased the average current density by a maximum of 7%, compared to an increase of 14% (higher conductivity) and 24% (higher buffer capacity) reported previously in a closed spacing MEC with a liquid catholyte.[35] The small impact of a higher substrate content, conductivity, and buffer capacity indicates that the MEC was likely limited by the electron transfer kinetics either at the anode or at the cathode at that specific cell voltage, and thus amending the anolyte with these chemicals resulted in a limited impact on the performance. A similar behavior has been reported on MFCs operating at a low current density when the rate of the reaction is controlled by the anode and cathode electron transfer rate.[11,39,40]

Hydrogen Gas Production Rates. The high current density of the vapor-fed MEC allowed record hydrogen production rates, while the AEM favored almost pure H$_2$ to be generated at the cathode (Figure 3A). The H$_2$ production rate increased from 35 ± 2 LH$_2$/L-d at an MEC voltage of 0.64 V (V_{app} = 0.8 V) to 72 ± 2 LH$_2$/L-d at 0.79 V (V_{app} = 1.1 V) in 50 mM PBS. The large hydrogen production rate was
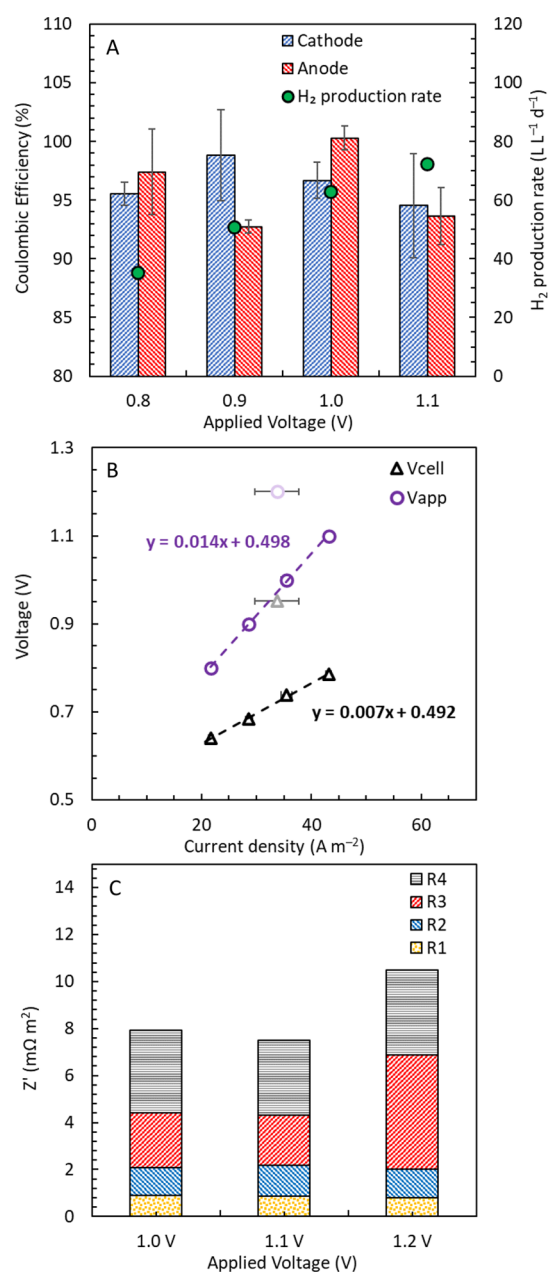

Figure 3. (A) Coulombic efficiencies for the anode and cathode at different applied voltages and the corresponding hydrogen generation rate. (B) MEC polarization curve based on the applied (V_{app}) or cell (V_{cell}) voltage for the vapor-fed cathode MEC. The dashed lines represent the linearization of the data in the linear current/voltage region. Faded data points were not included in the calculation of the MEC internal resistance from the slope. (C) Resistances calculated from the fitting of the EIS spectra at different applied voltages. EIS spectra and equivalent circuit are reported in the Supporting Information.

consistent with the current density of the MEC, with H$_2$ gas losses due to H$_2$ cycling to the anode minimized by the use of a membrane, which also enabled the production of high-purity gas.[41,42] No oxygen gas was detected in the cathode gas bag and headspace during continuous operation in the MEC at any voltage tested. The cathode coulombic efficiency (H$_2$ produced compared to the current) was larger than 90% for all the voltage applied and throughout the whole experiments (V_{app} = 0.80 V, CE = $96 \pm 1\%$; V_{app} = 0.90 V, CE = $99 \pm 4\%$;

V_{app} = 1.00 V, CE = 97 ± 2%; V_{app} = 1.10 V, CE = 95 ± 4%). The high cathode efficiency was likely due to the presence of a membrane separating the anode and cathode and the absence of a catholyte, which limits the growth of bacteria in the catholyte and in the cathode chamber,[16,37,43,44] and the high current density, which diminished the relative impact of H_2 leaking through the AEM compared to the overall H_2 produced.[45]

Electrochemical Analysis of the MEC. The high current density of the vapor-fed cathode MEC at each cell voltage was facilitated by the low internal resistance of the reactor (Figure 3B). The MEC internal resistances, calculated from the slope of V_{cell} or V_{app} at the different current densities, were 6.8 ± 0.3 mΩ m^2 (V_{cell}) and 14.0 ± 0.2 mΩ m^2 (V_{app}). The difference in these resistances was due to the external resistor (10 Ω) installed in series in the circuit of the MEC that was used to monitor the current, accounting for a loss of 7 mΩ m^2.[29] At the high current produced by the vapor-fed MEC (up to 30 mA), the voltage loss across the 10 Ω resistor was substantial, accounting for up to half of the applied voltage in addition to the onset voltage. Directly applying a voltage difference between the MEC terminals (no resistor) could avoid this loss, but it would not have allowed measurement of the MEC current density based on the voltage drop across the resistor.

The onset voltage can be approximated as the minimum voltage required to drive an electrochemical reaction, and it should be as close as possible to the thermodynamic equilibrium voltage calculated from the Nernst equation. The vapor-fed MEC onset voltage was 0.49 ± 0.01 V, implying that a minimum voltage difference of approximately 0.5 V should be applied between the anode and cathode to drive the electrochemical reaction at an appreciable rate, corresponding to a voltage 0.35 V higher than that calculated using the Nernst equation. This additional voltage includes the anode and cathode overpotentials and the concentration gradients.

The components of the overall MEC resistance were investigated with EIS at different applied voltages (Figure 3C). The smallest MEC internal resistance from the EIS analysis was 7.5 mΩ m^2 at V_{app} = 1.1 V, similar to that obtained from the slope of the polarization curve (6.8 ± 0.3 mΩ m^2). Four main resistances (R_{1-4}) were identified from the fitting of the spectra; the first two (R_{1-2}) did not appreciably change at different applied potentials and thus were not likely related to electron transfer processes and can be assumed to be due to ohmic resistances as previously reported.[11] R_1 was likely due to the resistance of the membrane and the electrolyte. R_2 was due to the inner porosity of the carbon felt anode and the Pt/C cathode, consistent with previous observations using porous electrodes.[11,46,47] R_1 and R_2 can be reduced by selecting thinner and more conductive membranes and by increasing the conductivity of the electrodes. The two remaining resistances (R_3 and R_4) showed large variability at the different applied voltages and thus can be ascribed to electron transport processes such as those happening at the anode and at the cathode. The anode and cathode resistances can be decreased by using more porous electrodes[48] and increase the activity of the cathode catalysts.[49] Unfortunately, space limitations in the zero-gap MEC and possible interference with the liquid flow path and electric field[19,21] did not allow insertion of a reference electrode to measure the individual electrode performance. Thus, it was not possible to identify the impact of the individual electrochemical reactions on the overall MEC internal resistance. However, the internal resistance was distributed between ohmic, anodic, and cathodic processes, with the ohmic resistance (2.2 mΩ m^2) contributing to 29% of the internal resistance and the anode and cathode for the remaining 71% (5.3 mΩ m^2). We have previously shown that the behavior of the electrode is completely different when assembled in the vapor-fed cathode configuration compared to other configurations in MFCs.[16] For example, the maximum anode current density was 6× larger in a vapor-fed cathode MFC than that in a 28 mL MFC due to favored transport of OH$^-$ in the anode in the vapor-fed configuration, which limited the acidification of the anodic biofilm and enabled higher anodic current densities. Thus, the electrode performance should be investigated in the relevant electrochemical configuration.

Impact of the Buffer Capacity on the Vapor-Fed MEC Performance. Increasing the buffer capacity from 50 to 100 mM increased the current density by only 7% at V_{app} = 1.1 V (Figure 2). To investigate the impact of the buffer capacity at different applied voltages, the concentration of the PBS of anolyte was varied (20, 50, or 100 mM) while applying several different cell voltages (Figure 4A and Figure S6). Increasing the buffer capacity of the anolyte produced higher limiting current densities. With 100 mM PBS, the limiting current density was 54 ± 1 A/m^2 at V_{cell} = 0.86 ± 0.02 V (V_{app} = 1.2 V) compared to 43.2 ± 1.1 A/m^2 (V_{cell} = 0.79 ± 0.00 V, V_{app} = 1.1 V) in 50 mM PBS. Decreasing the buffer capacity to 20
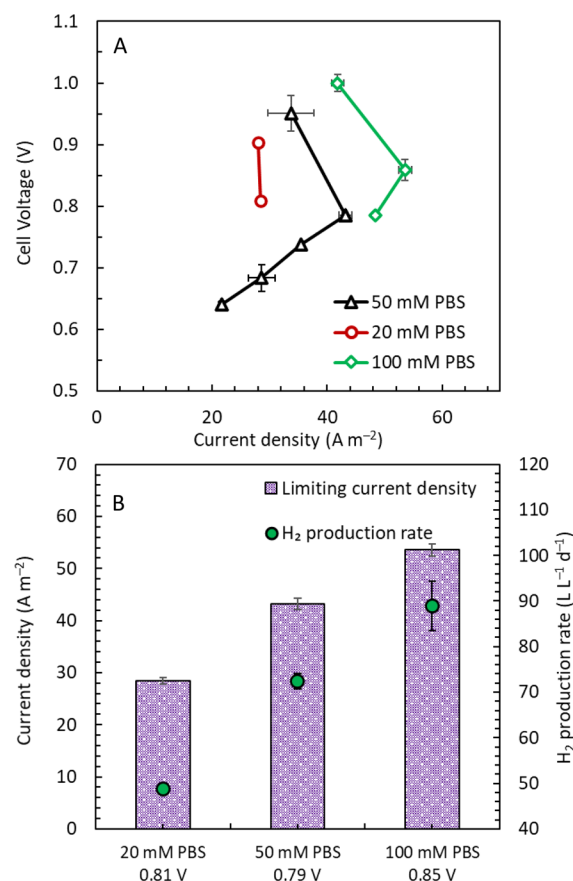

Figure 4. (A) MEC polarization curves as a function of the buffer capacity of the anolyte. (B) MEC performance in terms of average current density over a cycle at the maximum current density and hydrogen production rate using different buffer concentrations at the anode.

mM reduced the limiting current density to 28.5 ± 0.6 A/m^2 ($V_{cell} = 0.81 \pm 0.00$ V, $V_{app} = 1.0$ V) (Figure 4B). Thus, increasing the buffer capacity enabled higher limiting current densities at higher applied voltages by allowing a better control of the local anode pH.

The importance of the buffer capacity on the performance of bioelectrochemical systems is well known, but typically, it is only examined at a single fixed applied voltage or set electrode potential and it has not been examined in MECs without a catholyte.[9,11,35,50] Oxidation of substrates at the anode will generate one proton for each electron produced. If the protons are not effectively removed, then the solution near the anode will acidify, limiting the activity of the bacterial biofilm. Increasing the anolyte buffer concentration allows better control of the local anode pH, enabling higher current densities. The vapor-fed cathode MEC, due to its design with no catholyte, is effective in delivering OH$^-$ directly to the anode in close contact with the AEM; however, the transport from the membrane surface to the carbon felt pores is still controlled by diffusion and migration.[51] Thus, a concentration gradient can still exist within the anode 3D structure, leading to proton accumulation in certain areas of the biofilm. Previous studies have shown that the acidification of the biofilm in the pores is largely controlled by the buffer capacity of the solution and reducing the buffer concentration damaged the inner layer of the biofilm.[51,52]

Impact of a Liquid Feed Compared to the Vapor Cathode Feed on MEC Performance. To investigate the impact of feeding a liquid catholyte on MEC performance, a new MEC fed a 100 mM KCl catholyte was inoculated and operated at a similar V_{app} of the vapor-fed MEC (Figure S7). The 100 mM KCl-fed MEC produced a slightly lower current density compared to the vapor-fed MEC at each V_{app} (Figure 5A). For example, the average current density over a whole cycle in the vapor-fed MEC was 12% larger at $V_{app} = 0.9$ V (28.7 ± 2.3 A/m^2) and 8% larger at $V_{app} = 1.1$ V (43.2 ± 1.1 A/m^2) compared to the 100 mM KCl-fed MEC ($V_{app} = 0.9$ V, 25.6 ± 0.3 A/m^2; $V_{app} = 1.1$ V, 39.9 ± 0.6 A/m^2). The average current density produced by the 100 mM KCl fed MEC was higher compared to previously published results using similar electrolytes than that used here,[5,7,24,37] likely due to the small spacing between the anode and the cathode, which were separated only by the AEM. Reducing the spacing between the electrodes diminishes the ohmic resistance due to ion conductivity of the electrolytes, while narrowing the distance between where the protons and hydroxide ions are generated and consumed enables a better control of the local pH, as previously indicated.[9] The thin Pt/C catalyst layer likely limited the development of large concentration gradients in the cathode. A similar cathode to the one used here was shown to have a catalyst layer thickness of only 34.6 μm.[16]

The conductivity, buffer concentration, and pH of the liquid catholyte used in the MECs were changed over time to investigate their impact on MEC performance relative to vapor-fed cathodes (Figure 5B,C). Using a salty solution of 50 mM KCl (40.5 ± 0.2 A/m^2, $\sigma = 7$ mS/cm) produced lower current densities than those obtained with the vapor cathode (42.7 ± 0.5 A/m^2). The presence of the salt in the liquid reduced performance by enabling the transport of Cl$^-$ to the anode to balance charge rather than only OH$^-$ ions, as evidenced by the rapid increase in catholyte pH. After only 1 day of operation using KCl, the catholyte pH increased to 11.1. This increase in pH was due to transfer of Cl$^-$ through the
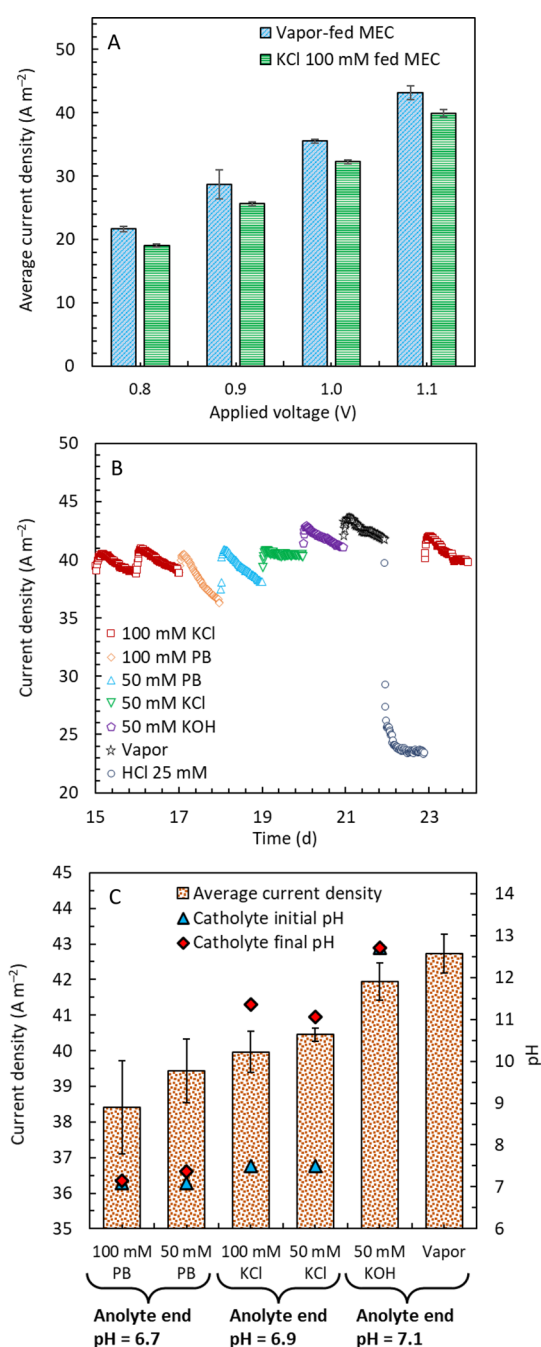

Figure 5. (A) Comparison of the MEC performance at different applied voltages in the vapor-fed and in the liquid-fed MEC. (B) Performance of the liquid-fed cathode MEC using 100 mM KCl, 100 mM PB, 50 mM PB, 50 mM KOH, and 25 mM HCl at $V_{app} = 1.1$ V and (C) corresponding average current density and solution pH.

AEM, resulting in less transfer of OH$^-$ to the anode, which adversely impacted the anode performance by lowering the anode pH. Increasing the Cl$^-$ concentration from 50 to 100 mM KCl ($\sigma = 14$ mS/cm) further reduced the current density (40.0 ± 0.6 A/m^2) as this would favor increased chloride ion transport to the anode and thus less OH$^-$ ions. Approximately 11% of the charge was balanced by Cl$^-$ with 100 mM KCl compared to 5% with 50 mM KCl based on the catholyte pH increase.

Buffering the catholyte reduced MEC performance to 39.4 ± 0.9 A/m^2 using 50 mM PBS ($\sigma = 6$ mS/cm) and 38.4 ± 1.3 A/

m^2 with 100 mM PB (σ = 11 mS/cm). This reduction was due to the transport of phosphate ions to the anode through the AEM for balancing charge, rather than any improvement in HER kinetics due to the lower cathode pH. Adding the buffer to the catholyte limited the increase in pH, which thermodynamically should improve the driving potential for the HER. However, the addition of phosphate ions (50 or 100 mM) in the buffer resulted in a much higher concentration of phosphate anions than hydroxide ions (0.1 μM) at a near-neutral pH. Thus, addition of the buffer reduced the mass transport of OH$^-$ needed to balance the anode pH, resulting in a decrease in the current density compared to that possible with only the vapor cathode.

Using an acidic catholyte did not improve current densities relative to the vapor-fed cathode. With an acid catholyte produced by using 25 mM HCl (pH = 1.6, σ = 11 mS/cm), the current density was substantially reduced to only 24.3 $\pm$ 2.1 A/m^2 compared to 42.7 $\pm$ 0.5 A/m^2 with a vapor-fed cathode. Addition of HCl greatly increased the concentration of Cl$^-$ compared to OH$^-$, which resulted in the charge transport balanced primarily by the transfer of Cl$^-$ ions to the anode, rather than OH$^-$ ions. Thus, while the low catholyte pH could be predicted to increase the potential for driving the HER, there was no increased current due to the more favorable Cl$^-$ ion transport, which adversely impacts the anode performance. According to the change in pH of the catholyte, 84% of the charge transported to the anode over a 1 day cycle would have been due to chloride ions with HCl as a catholyte, consistent with an observed large decrease in the catholyte conductivity from 11.3 to 8.4 mS/cm. Operation under these conditions did not adversely impact the stability of the biofilm, as seen by a return to the previous current density when the HCl cathode feed was switched back to a plain salt (100 mM KCl) (Figure 5B).

Using an alkaline liquid catholyte, pH did not improve current densities compared to a vapor feed. With 50 mM KOH (pH = 12.7, σ = 12 mS/cm), the average current density over a 1 day cycle was 41.9 $\pm$ 0.5 A/m^2, similar to that of the vapor-fed system (42.7 $\pm$ 0.5 A/m^2). Since the high current density depended on OH$^-$ ion transport, the presence of a high concentration of these ions at a pH of 12.7 should have been favorable for mass transport of these ions. The lack of an increase in the current could have been offset by leakage of positive charge from the anolyte into the catholyte to balance charge. Some cation transport can occur through an AEM because ion exchange membranes are not 100% permselective. Although the use of an alkaline liquid catholyte could produce very similar current densities to the vapor anode, the need to add base solutions is not preferred over the vapor catholyte due to the cost of adding and handling that chemical. The energy needed to produce the water vapor was much lower (43% less) than the energy needed to apply a cell voltage of 0.79 V to the MEC, resulting in minimal additional energy.

These results with the different catholytes show that the vapor-fed catholyte improved performance of the zero-gap MEC except when a strongly alkaline catholyte was used. Catholytes with salts or buffers and acidic catholytes, which add high concentrations of anions to balance charge, should be avoided. For this MEC configuration to improve current generation, it is important to create conditions that avoid competition of ion transport by species other than hydroxide ions. With a vapor-fed cathode or a highly alkaline catholyte, only OH$^-$ ions are transported from the cathode to anode to balance electron transfer, resulting in similar initial and final anolyte and catholyte pH levels.

Advantages of a Vapor-Fed Cathode Compared to a Liquid Catholyte in MECs. The zero-gap design combined with the vapor-fed cathode configuration produced the best MEC performance to date. The high current density was enabled by several innovative aspects of the design compared to conventional MECs with a liquid catholyte. The zero-gap spacing decreased the ohmic resistance to only 2.2 mΩ m^2 compared to 14 mΩ m^2 previously reported in a 28 mL reactor with 1 cm spacing between the electrodes using the same electrolyte.[6] Reducing the spacing allowed effective hydroxide ion transport compared to other chemical species, favoring a more neutral anode pH,[12] as protons generated at the anode can limit the current density produced in MECs by reducing the local pH.[5,9] The pH range tolerated by the bioanode is typically constrained to a change of only a few units of pH around neutrality. The activity of the biofilm on the anode is drastically diminished when the pH decreases below neutral.[53] It was previously reported that the diffusion layer thickness of protons in a brush bioanode was approximately 290 $\pm$ 30 μm,[11] and thus, reducing the electrode spacing using an AEM that was 100 μm thick between the anode and cathode expedited the neutralization of H$^+$/OH$^-$ generated at the electrodes.

The AEM and the absence of a catholyte in the vapor-fed cathode MEC enabled a high current density by facilitating the selective transport of hydroxide ions directly next to the anode felt, neutralizing the protons generated from the substrate oxidation reaction. It was previously reported that OH$^-$ are the main species transported across an AEM only when the catholyte pH increases to approximately 13.[5,34,54] This is due to the competition between the transport of other ions in the solution, such as Cl$^-$, which are typically more concentrated than OH$^-$ at pH 7 and are used to maintain a high solution conductivity of the catholyte. Thus, as soon as the electrons reach the cathode, the AEM enables anion transport from the cathode to the anode to balance the charge due to electron transport and maintain electroneutrality. For a 100 mM KCl solution at pH 7, primarily Cl$^-$ will diffuse from the cathode to anode until the catholyte pH, due to the production of OH$^-$ by the HER, increases to approximately 13. After that point, mainly OH$^-$ will diffuse from the cathode to anode.[34,54] If the catholyte volume is decreased, for example, from a few milliliter to a few microliter, then the moles of Cl$^-$ diffusing to the anode will be 1000$\times$ less, limiting excessive acidification of the anode biofilm and allowing the bioanode to deliver a larger current density. In the vapor-fed MEC, no catholyte is fed to the cathode, while its ionic conductivity is ensured by the ion exchange polymer dispersed in the catalyst layer and the AEM. Thus, the acidification of the anode pressed against the AEM is substantially decreased as the OH$^-$ produced at the cathode are the only ions that can be transported to the anode, neutralizing the protons generated by the bioanode. In the best case scenario, in the vapor-fed cathode MEC, no ions are present in the cathode chamber at any point and only the water from the vapor or diffusing through the membrane is consumed by the HER, while the AEM enables the transport of OH$^-$ across the membrane as soon as they are generated. However, ion exchange membranes are never 100% selective, and small amount of co-ions (ions of the same charge of the membrane) can leak through the membrane; moreover, due to the concentration difference, a small volume of solution can

leak from the anode to the cathode, even though the anion transport is limited by the electrons (negatively charged) flowing in the same direction. In any case, even though a pH gradient might still exist across the membrane, potentially due to the unselective AEM and anion leakage, the negligible volume of the catholyte prevents excessive acidification of the anode in contact with the AEM.

The vapor-fed MEC design using an AEM has several advantages compared to previous MEC configurations and operating conditions, including the use of the vapor feed (humidified gas feed) to keep the cathode from drying out as well as avoiding H_2 bubble formation in a liquid catholyte, using an AEM rather than a cation exchange membrane (CEM), and flow through the anode. Four previous studies used gas-cathodes (a gas phase not containing water vapor),[45,55−57] but these different configurations had sub-optimal designs compared to our vapor-fed cathode design with an AEM (Table S1). In three of these studies, a CEM was used to separate the anode and cathode.[55−57] This configuration would result in transport through the CEM of cations other than protons due to their differences in concentration, resulting in pH imbalances. Here, the hydroxide ions are transported from the cathode as the main reaction at the cathode is water dissociation to release OH^- ions.[58] It was previously reported that a CEM enables charge balance primarily by transport of sodium and magnesium in a vapor-cathode MFC, producing 3 times less power than a vapor-fed cathode MFC using an AEM due to anode acidification.[16] Additionally, in one of these studies,[55] the anode was placed 3 mm from the membrane, favoring the development of a local pH gradient and adding additional ohmic losses to the cell. In another gas-phase cathode study, an AEM was used,[45] but the anode, cathode, and AEM were not pressed against each other, which could have allowed liquid to accumulate between the electrodes, resulting in pH decreases in the solution near the anode. Also, the anolyte was not flowing through the anode, which could lead to substrate limitations as well as lower local pH conditions. Moreover, the cathode catalyst preparation was different from that used here, which also could reduce performance. As a result of these different configurations, these two different designs produced much lower maximum current densities (<5 A/m^2)[45,55] than those obtained here.

The vapor-fed cathode MEC developed here performed significantly better than other liquid catholyte studies, and it improved reactor stability and longevity. For example, a maximum current density of 22.8 ± 0.1 A/m^2 was previously obtained using a 0.1 M KCl-fed catholyte at a cell voltage of 1.0 V after 2 weeks of operation. Even though there were some similar conditions in that study compared to those here (anode felt, HRT: ∼10/15 s), the maximum current density of the vapor-fed MEC was 36% larger (31 ± 1 A/m^2 at 0.80 ± 0.01 V) using the 20 mM PBS anolyte compared to 10 mM in that study. Most importantly the current density in that study could not be sustained over time due to scaling of the membrane. Here, the vapor-fed MEC was continuously operated for up to 50 days under different operational conditions and no scaling was observed when the reactor was disassembled (Figure S9). Other advantages of the vapor-fed cathode MEC includes the possibility of pressurizing the H_2 gas in the cathode chamber,[4] lowering opportunities for cathode catalyst leaching or dissolution due to the absence of liquid flow, no production of caustic solutions at the cathode, lower energy requirements due to reduced pumping energy for a gas rather than a liquid,

and a lower impact of gas bubble evolution on the reduction of the electroactive area at the cathode.[5,7] Thus, the vapor-fed design can help improve performance, achieve greater stability over time, and reduce cathode fouling, factors that have been detrimental to implementation of MECs for practical applications.

■ ASSOCIATED CONTENT

ⓢ Supporting Information

The Supporting Information is available free of charge at https://pubs.acs.org/doi/10.1021/acs.est.1c06769.

> Impact of catholyte pH on the HER potential, comparison between performance of the MEC fed daily for or only once over 3 days of operation, EIS spectra, impact of solution chemistry on the performance, impact of buffer capacity on limiting current density, comparison of three independent runs of duplicate MEC operating under similar conditions, and photos of the electrodes and MEA at the end of the experiment (PDF)

■ AUTHOR INFORMATION

Corresponding Author

　Ruggero Rossi − *Department of Civil and Environmental Engineering, The Pennsylvania State University, University Park, Pennsylvania 16802, United States;* ⓞ orcid.org/0000-0002-3807-3980; Email: rxr57@psu.edu

Authors

　Gahyun Baek − *Department of Civil and Environmental Engineering, The Pennsylvania State University, University Park, Pennsylvania 16802, United States;* ⓞ orcid.org/0000-0002-3707-5300
　Bruce E. Logan − *Department of Civil and Environmental Engineering, The Pennsylvania State University, University Park, Pennsylvania 16802, United States;* ⓞ orcid.org/0000-0001-7478-8070

Complete contact information is available at:
https://pubs.acs.org/10.1021/acs.est.1c06769

Author Contributions

R.R. and B.E.L. designed research and planned experiments, R.R. performed experiments, and all authors analyzed data and contributed to writing the final version of the paper.

Notes

The authors declare no competing financial interest.

■ REFERENCES
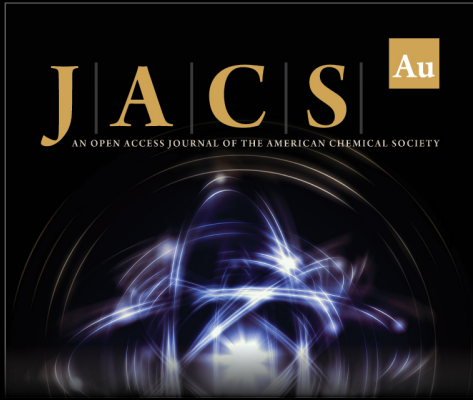
(1) Foley, J. M.; Rozendal, R. A.; Hertle, C. K.; Lant, P. A.; Rabaey, K. Life Cycle Assessment of High-Rate Anaerobic Treatment, Microbial Fuel Cells, and Microbial Electrolysis Cells. *Environ. Sci. Technol.* 2010, 44, 3629−3637.

(2) Logan, B. E.; Call, D.; Cheng, S.; Hamelers, H. V. M.; Sleutels, T. H. J. A.; Jeremiasse, A. W.; Rozendal, R. A. Microbial Electrolysis Cells for High Yield Hydrogen Gas Production from Organic Matter. *Environ. Sci. Technol.* 2008, 42, 8630−8640.

(3) Lee, H. S.; Vermaas, W. F. J.; Rittmann, B. E. Biological Hydrogen Production: Prospects and Challenges. *Trends Biotechnol.* 2010, 28, 262−271.

(4) Rousseau, R.; Etcheverry, L.; Roubaud, E.; Basséguy, R.; Délia, M. L.; Bergel, A. Microbial Electrolysis Cell (MEC): Strengths, Weaknesses and Research Needs from Electrochemical Engineering Standpoint. *Appl. Energy* **2020**, *257*, 113938.

(5) Ki, D.; Popat, S. C.; Torres, C. I. Reduced Overpotentials in Microbial Electrolysis Cells through Improved Design, Operation, and Electrochemical Characterization. *Chem. Eng. J.* **2016**, *287*, 181−188.

(6) Rossi, R.; Cario, B. P.; Santoro, C.; Yang, W.; Saikaly, P. E.; Logan, B. E. Evaluation of Electrode and Solution Area-Based Resistances Enables Quantitative Comparisons of Factors Impacting Microbial Fuel Cell Performance. *Environ. Sci. Technol.* **2019**, *53*, 3977−3986.

(7) Jeremiasse, A. W.; Hamelers, H. V. M.; Saakes, M.; Buisman, C. J. N. Ni Foam Cathode Enables High Volumetric H_2 Production in a Microbial Electrolysis Cell. *Int. J. Hydrogen Energy* **2010**, *35*, 12716−12723.

(8) Ruiz, Y.; Baeza, J. A.; Guisasola, A. Enhanced Performance of Bioelectrochemical Hydrogen Production Using a PH Control Strategy. *ChemSusChem* **2015**, *8*, 389−397.

(9) Popat, S. C.; Torres, C. I. Critical Transport Rates That Limit the Performance of Microbial Electrochemistry Technologies. *Bioresour. Technol.* **2016**, *215*, 265−273.

(10) Rozendal, R. A.; Hamelers, H. V. M.; Buisman, C. J. N. Effects of Membrane Cation Transport on PH and Microbial Fuel Cell Performance. *Environ. Sci. Technol.* **2006**, *40*, 5206−5211.

(11) Rossi, R.; Hall, D. M.; Wang, X.; Regan, J. M.; Logan, B. E. Quantifying the Factors Limiting Performance and Rates in Microbial Fuel Cells Using the Electrode Potential Slope Analysis Combined with Electrical Impedance Spectroscopy. *Electrochim. Acta* **2020**, *348*, 136330.

(12) Torres, C. I.; Marcus, A. K.; Rittmann, B. E. Proton Transport inside the Biofilm Limits Electrical Current Generation by Anode-Respiring Bacteria. *Biotechnol. Bioeng.* **2008**, *100*, 872−881.

(13) Popat, S. C.; Ki, D.; Rittmann, B. E.; Torres, C. I. Importance of OH^- Transport from Cathodes in Microbial Fuel Cells. *ChemSusChem* **2012**, *5*, 1071−1079.

(14) Nam, J. Y.; Logan, B. E. Enhanced Hydrogen Generation Using a Saline Catholyte in a Two Chamber Microbial Electrolysis Cell. *Int. J. Hydrogen Energy* **2011**, *36*, 15105−15110.

(15) Ye, Y.; Logan, B. E. The Importance of OH^- Transport through Anion Exchange Membrane in Microbial Electrolysis Cells. *Int. J. Hydrogen Energy* **2018**, *43*, 2645−2653.

(16) Rossi, R.; Logan, B. E. Using an Anion Exchange Membrane for Effective Hydroxide Ion Transport Enables High Power Densities in Microbial Fuel Cells. *Chem. Eng. J.* **2021**, *422*, 130150.

(17) Liu, Z.; Wainright, J. S.; Huang, W.; Savinell, R. F. Positioning the Reference Electrode in Proton Exchange Membrane Fuel Cells: Calculations of Primary and Secondary Current Distribution. *Electrochim. Acta* **2004**, *49*, 923−935.

(18) Chan, S. H.; Chen, X. J.; Khor, K. A. Reliability and Accuracy of Measured Overpotential in a Three-Electrode Fuel Cell System. *J. Appl. Electrochem.* **2001**, *31*, 1163−1170.

(19) He, W.; Van Nguyen, T. Edge Effects on Reference Electrode Measurements in PEM Fuel Cells. *J. Electrochem. Soc.* **2004**, *151*, A185.

(20) Adler, S. B. Reference Electrode Placement in Thin Solid Electrolytes. *J. Electrochem. Soc.* **2002**, *149*, E166.

(21) Eccarius, S.; Manurung, T.; Ziegler, C. On the Reliability of Measurements Including a Reference Electrode in DMFCs. *J. Electrochem. Soc.* **2007**, *154*, B852.

(22) Feng, Y.; Yang, Q.; Wang, X.; Logan, B. E. Treatment of Carbon Fiber Brush Anodes for Improving Power Generation in Air-Cathode Microbial Fuel Cells. *J. Power Sources* **2010**, *195*, 1841−1844.

(23) Rossi, R.; Wang, X.; Logan, B. E. High Performance Flow through Microbial Fuel Cells with Anion Exchange Membrane. *J. Power Sources* **2020**, *475*, 228633.

(24) Sleutels, T. H. J. A.; Hamelers, H. V. M.; Buisman, C. J. N. Effect of Mass and Charge Transport Speed and Direction in Porous

Anodes on Microbial Electrolysis Cell Performance. *Bioresour. Technol.* **2011**, *102*, 399−403.

(25) Lee, H.-S.; Torres, C. I.; Rittmann, B. E. Effects of Substrate Diffusion and Anode Potential on Kinetic Parameters for Anode-Respiring Bacteria. *Environ. Sci. Technol.* **2009**, *43*, 7571−7577.

(26) Cheng, S.; Xing, D.; Call, D. F.; Logan, B. E. Direct Biological Conversion of Electrical Current into Methane by Electromethanogenesis. *Environ. Sci. Technol.* **2009**, *43*, 3953−3958.

(27) Kadier, A.; Simayi, Y.; Kalil, M. S.; Abdeshahian, P.; Hamid, A. A. A Review of the Substrates Used in Microbial Electrolysis Cells (MECs) for Producing Sustainable and Clean Hydrogen Gas. *Renewable Energy* **2014**, *71*, 466−472.

(28) Lu, L.; Ren, Z. J. Microbial Electrolysis Cells for Waste Biorefinery: A State of the Art Review. *Bioresour. Technol.* **2016**, *215*, 254−264.

(29) Cario, B. P.; Rossi, R.; Kim, K. Y.; Logan, B. E. Applying the Electrode Potential Slope Method as a Tool to Quantitatively Evaluate the Performance of Individual Microbial Electrolysis Cell Components. *Bioresour. Technol.* **2019**, *287*, 121418.

(30) Logan, B. E.; Zikmund, E.; Yang, W.; Rossi, R.; Kim, K.-Y.; Saikaly, P. E.; Zhang, F. Impact of Ohmic Resistance on Measured Electrode Potentials and Maximum Power Production in Microbial Fuel Cells. *Environ. Sci. Technol.* **2018**, *52*, 8977−8985.

(31) Ambler, J. R.; Logan, B. E. Evaluation of Stainless Steel Cathodes and a Bicarbonate Buffer for Hydrogen Production in Microbial Electrolysis Cells Using a New Method for Measuring Gas Production. *Int. J. Hydrogen Energy* **2011**, *36*, 160−166.

(32) Logan, B. E.; Hamelers, B.; Rozendal, R.; Schröder, U.; Keller, J.; Freguia, S.; Aelterman, P.; Verstraete, W.; Rabaey, K. Microbial Fuel Cells: Methodology and Technology. *Environ. Sci. Technol.* **2006**, *40*, 5181−5192.

(33) Tartakovsky, B.; Mehta, P.; Santoyo, G.; Guiot, S. R. Maximizing Hydrogen Production in a Microbial Electrolysis Cell by Real-Time Optimization of Applied Voltage. *Int. J. Hydrogen Energy* **2011**, *36*, 10557−10564.

(34) Sleutels, T. H. J. A.; Ter Heijne, A.; Buisman, C. J. N.; Hamelers, H. V. M. Steady-State Performance and Chemical Efficiency of Microbial Electrolysis Cells. *Int. J. Hydrogen Energy* **2013**, *38*, 7201−7208.

(35) Sleutels, T. H. J. A.; Lodder, R.; Hamelers, H. V. M.; Buisman, C. J. N. Improved Performance of Porous Bio-Anodes in Microbial Electrolysis Cells by Enhancing Mass and Charge Transport. *Int. J. Hydrogen Energy* **2009**, *34*, 9655−9661.

(36) Baek, G.; Rossi, R.; Logan, B. E. Changes in Electrode Resistances and Limiting Currents as a Function of Microbial Electrolysis Cell Reactor Configurations. *Electrochim. Acta* **2021**, *388*, 138590.

(37) Rousseau, R.; Ketep, S. F.; Etcheverry, L.; Délia, M. L.; Bergel, A. Microbial Electrolysis Cell (MEC): A Step Ahead towards Hydrogen-Evolving Cathode Operated at High Current Density. *Bioresour. Technol. Reports* **2020**, *9*, 100399.

(38) Chen, S.; He, G.; Liu, Q.; Harnisch, F.; Zhou, Y.; Chen, Y.; Hanif, M.; Wang, S.; Peng, X.; Hou, H.; Schröder, U. Layered Corrugated Electrode Macrostructures Boost Microbial Bioelectrocatalysis. *Energy Environ. Sci.* **2012**, *5*, 9769−9772.

(39) Rossi, R.; Logan, B. E. Impact of External Resistance Acclimation on Charge Transfer and Diffusion Resistance in Bench-Scale Microbial Fuel Cells. *Bioresour. Technol.* **2020**, *318*, 123921.

(40) Kook, L.; Nemestóthy, N.; Bélafi-Bakó, K.; Bakonyi, P. Investigating the Specific Role of External Load on the Performance versus Stability Trade-off in Microbial Fuel Cells. *Bioresour. Technol.* **2020**, *309*, 123313.

(41) Rago, L.; Ruiz, Y.; Baeza, J. A.; Guisasola, A.; Cortés, P. Microbial Community Analysis in a Long-Term Membrane-Less Microbial Electrolysis Cell with Hydrogen and Methane Production. *Bioelectrochemistry* **2015**, *106*, 359−368.

(42) Montpart, N.; Rago, L.; Baeza, J. A.; Guisasola, A. Hydrogen Production in Single Chamber Microbial Electrolysis Cells with Different Complex Substrates. *Water Res.* **2015**, *68*, 601−615.

(43) Wang, A.; Liu, W.; Cheng, S.; Xing, D.; Zhou, J.; Logan, B. E. Source of Methane and Methods to Control Its Formation in Single Chamber Microbial Electrolysis Cells. *Int. J. Hydrogen Energy* **2009**, *34*, 3653−3658.

(44) Wang, L.; Liu, W.; He, Z.; Guo, Z.; Zhou, A.; Wang, A. Cathodic Hydrogen Recovery and Methane Conversion Using Pt Coating 3D Nickel Foam Instead of Pt-Carbon Cloth in Microbial Electrolysis Cells. *Int. J. Hydrogen Energy* **2017**, *42*, 19604−19610.

(45) Rozendal, R. A.; Hamelers, H. V. M.; Molenkmp, R. J.; Buisman, J. N. Performance of Single Chamber Biocatalyzed Electrolysis with Different Types of Ion Exchange Membranes. *Water Res.* **2007**, *41*, 1984−1994.

(46) Ahn, S.; Tatarchuk, B. J. Air Electrode: Identification of Intraelectrode Rate Phenomena via AC Impedance. *J. Electrochem. Soc.* **1995**, *142*, 4169.

(47) Alcaide, F.; Brillas, E.; Cabot, P. L. EIS Analysis of Hydroperoxide Ion Generation in an Uncatalyzed Oxygen-Diffusion Cathode. *J. Electroanal. Chem.* **2003**, *547*, 61−73.

(48) He, G.; Gu, Y.; He, S.; Schröder, U.; Chen, S.; Hou, H. Effect of Fiber Diameter on the Behavior of Biofilm and Anodic Performance of Fiber Electrodes in Microbial Fuel Cells. *Bioresour. Technol.* **2011**, *102*, 10763−10766.

(49) Kim, K. Y.; Yang, W.; Logan, B. E. Regenerable Nickel-Functionalized Activated Carbon Cathodes Enhanced by Metal Adsorption to Improve Hydrogen Production in Picrobial Electrolysis Cells. *Environ. Sci. Technol.* **2018**, *52*, 7131−7137.

(50) Bond, D. R.; Strycharz-Glaven, S. M.; Tender, L. M.; Torres, C. I. On Electron Transport through Geobacter Biofilms. *ChemSusChem* **2012**, *5*, 1099−1105.

(51) Chong, P.; Erable, B.; Bergel, A. Microbial Anodes: What Actually Occurs inside Pores? *Int. J. Hydrogen Energy* **2019**, *44*, 4484−4495.

(52) Chong, P.; Erable, B.; Bergel, A. Effect of Pore Size on the Current Produced by 3-Dimensional Porous Microbial Anodes: A Critical Review. *Bioresour. Technol.* **2019**, *289*, 121641.

(53) He, Z.; Huang, Y.; Manohar, A. K.; Mansfeld, F. Effect of Electrolyte pH on the Rate of the Anodic and Cathodic Reactions in an Air-Cathode Microbial Fuel Cell. *Bioelectrochemistry* **2008**, *74*, 78−82.

(54) Sleutels, T. H. J. A.; ter Heijne, A.; Kuntke, P.; Buisman, C. J. N.; Hamelers, H. V. M. Membrane Selectivity Determines Energetic Losses for Ion Transport in Bioelectrochemical Systems. *ChemistrySelect* **2017**, *2*, 3462−3470.

(55) Tartakovsky, B.; Manuel, M. F.; Neburchilov, V.; Wang, H.; Guiot, S. R. Biocatalyzed Hydrogen Production in a Continuous Flow Microbial Fuel Cell with a Gas Phase Cathode. *J. Power Sources* **2008**, *182*, 291−297.

(56) Satinover, S. J.; Schell, D.; Borole, A. P. Achieving High Hydrogen Productivities of 20 L/L-Day via Microbial Electrolysis of Corn Stover Fermentation Products. *Appl. Energy* **2020**, *259*, 114126.

(57) Satinover, S. J.; Rodriguez, M.; Borole, A. P. Microbial Electrolysis Cell Recovery after Inducing Operational Failure Conditions. *Biochem. Eng. J.* **2020**, *164*, 107800.

(58) Zhou, Z.; Pei, Z.; Wei, L.; Zhao, S.; Jian, X.; Chen, Y. Electrocatalytic Hydrogen Evolution under Neutral pH Conditions: Current Understandings, Recent Advances, and Future Prospects. *Energy Environ. Sci.* **2020**, *13*, 3185−3206.